

Synthesis, Crystal Structure and Reducibility of K_2NiF_4 Type Oxides $Sm_{2-x}Sr_xCuO_4$

ZHU, Ying-Hong(朱英红) LOU, Hui*(楼辉) LIU, Jia-Geng(刘加庚) LIU, Xue-Jian(刘学建)
MA, Fu-Tai(马福泰)

Department of Chemistry, Zhejiang University, Hangzhou, Zhejiang 310028, China

K_2NiF_4 type compounds $Sm_{2-x}Sr_xCuO_4$ ($0 \leq x \leq 1.2$) were prepared. Rietveld refinement of powder diffraction data shows that the crystal system of these compounds belongs to T' type tetragonal structure of space group $I4/mmm$, and the addition of Sr causes a dramatic shift of the O(I) ions along the c axis from Sm (Sr) toward Cu while scarcely affecting the Cu—O (II) bond in basal CuO_4 plane. From XRD data, it can be seen that when $0.0 \leq x \leq 0.6$, $Sm_{2-x}Sr_xCuO_4$ belongs to a single-phase K_2NiF_4 type structure, while at $x \geq 0.7$, both the free SrO phase and the CuO phase exist in these compounds. From the results of XPS and Rietveld refinement, it can be seen that after replacing Sm^{3+} with Sr^{2+} of lower valence, the valence of Cu and Sm does not change apparently, and thus some defect must be formed at the oxygen ion positions and/or position A on A_2BO_4 to keep charge balance and to stabilize the structure.

Keywords K_2NiF_4 type structure, $Sm_{2-x}Sr_xCuO_4$ compound, Rietveld refinement

Introduction

In recent years, K_2NiF_4 type compounds of rare earth complexes A_2BO_4 , consisting of alternating layers of ABO_3 perovskite and AO rock salt structures along c -axis, are widely studied due to their high temperature stability, two-dimensional conductivity, special electro-magnetic property and the catalytic activity for both oxidation and reduction.¹⁻⁵ These properties are closely related to the species of A and B, the valence state of the transition metal ions of B, as well as the crystal structure of the

compound.

According to the structure proposed by Joseph *et al.*,⁶ there are three kinds of structure, T, T' and T* existed in Ln_2CuO_4 compounds. Among them, La_2CuO_4 belongs to T structure where Cu is coordinated with 6 oxygen ions, Ln_2CuO_4 (Ln: Pr, Nd, Sm, Eu and Gd) are T' structure where Cu coordinates with 4 oxygen ions, while T* structure, where Cu is coordinated with 5 oxygen ions, is formed due to competition between T and T' structure. The preparation and structure characterization of $La_{2-x}Sr_xCuO_4$ have been reported.⁷⁻⁹ Bularzik⁷ suggested that the preparation conditions have little effect on the lattice parameters, but greatly affect the oxygen content of the compounds. Nguyen *et al.*⁸ reported that the crystal system of the compounds with $x \leq 0.1$ belongs to orthorhombic system, while compounds with x between 0.1 and 1.34 belong to tetragonal system. He⁹ pointed out that for the compounds of $La_{2-x}Sr_xCuO_4$, when $x = 0$, an orthorhombic $Fmmm$ structure forms and when $0.05 \leq x \leq 0.2$, the compounds belong to tetragonal $I4/mmm$. By controlling the content of Sr^{2+} , the amount of defect formed at A and B position can be adjusted. It is very interesting that such compounds reveal high catalytic activity both for oxidation of CO and reduction of NO_x .

We now wish to report the synthesis, crystal structure and reducibility of K_2NiF_4 type oxides $Sm_{2-x}SrCuO_4$ and discuss the effects of Sr substitution on the structure parameters.

* E-mail: louhui@163.net

Received June 7, 2001; revised September 17, 2001; accepted December 28, 2001.

Project supported by the Natural Science Foundation of Zhejiang Province (No. 292033).

Experimental

Preparation of $\text{Sm}_{2-x}\text{Sr}_x\text{CuO}_4$

The $\text{Sm}_{2-x}\text{Sr}_x\text{CuO}_4$ samples ($x = 0, 0.1, 0.2, 0.3, 0.4, 0.5, 0.6, 0.7, 0.8 \sim 1.2$) were prepared by a citric acid complex decomposition method.¹⁰ Briefly, an aqueous solution of mixed metal nitrates with an equivalent amount of citric acid was evaporated at 332–352 K to form a gel. The precursors were then decomposed at 923 K for 4 h, followed by grinding, pelletizing and calcining in air at 1473 K for 10 h.

Crystal structure characterization of $\text{Sm}_{2-x}\text{Sr}_x\text{CuO}_4$

XRD measurement

XRD data for Rietveld refinement were collected on a Rigaku D/max-III_B model with Bragg-Brentano geometry using graphite-monochromated Cu K_α radiation (40 kV \times 30 mA) and a scintillation detector. The intensity data were collected at 298 K over a 2θ range of 10° – 140° with a step interval of 0.04 and a counting time of 8 s per step. The d-spacings were corrected for systematic errors by calibration using standard silicon powder ($a = 0.54309$ nm), and the cell parameters were calculated using the least square method. The crystal system of the sample was determined using comparison of the diffraction patterns of the samples with that recorded in the category. The Rietveld refinement was performed using a program WYRLET (M. Schneider, a modified version of the program by Wiles and Young, 1981)¹¹. The starting model used in the refinement was the space group $Fm\bar{3}m$ or $I4/m\bar{3}m$ with structural parameters of a K_2NiF_4 type compound. Peaks were modeled using the pseudo-Voigt profile function in which a peak asymmetry parameter was included for peaks up to $2\theta = 50^\circ$. The background parameters were modeled using a refinable fourth-order polynomial. The occupation number of atoms for all sites was fixed and not refined.

IR measurement

The IR spectra were taken on a Perkin-Elmer 683 spectrophotometer. Samples were prepared in the form of KBr pellets.

DTA measurement

The initial temperature to form the $\text{Sm}_{2-x}\text{Sr}_x\text{CuO}_4$ compounds was determined by means of DTA method. The samples were exposed to stationary oxygen. The temperature range was from room temperature to 1473 K and the heating rate was 10 $^\circ\text{C}/\text{min}$.

Temperature-programmed reduction (TPR) of compounds

Samples of $\text{Sm}_{2-x}\text{Sr}_x\text{CuO}_4$ (about 5 mg) were placed in a quartz reactor, which was connected to a conventional TPR apparatus. The reduction stream used was composed of 10% (V/V) hydrogen in nitrogen (at a flow-rate of 20 mL/min). During the TPR measurement, the reactor was heated from room temperature to 1173 K at a heating rate of 20 K/min.

Results and discussion

Optimum temperature to form $\text{Sm}_{1.5}\text{Sr}_{0.5}\text{CuO}_4$ compounds

The DTA curve of $\text{Sm}_{1.5}\text{Sr}_{0.5}\text{CuO}_4$ sample calcined at 923 K for 4 h is shown in Fig. 1. There are two endothermic peaks at 1362 K and 1400 K, respectively. It seems that the formation temperature of $\text{Sm}_{1.5}\text{Sr}_{0.5}\text{CuO}_4$ compound is between 1362 K and 1400 K.

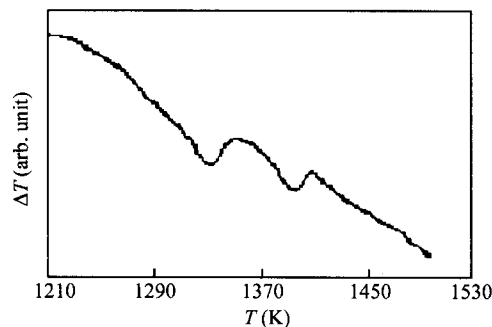


Fig. 1 DTA profile of $\text{Sm}_{1.5}\text{Sr}_{0.5}\text{CuO}_4$.

The XRD patterns of Sm_2CuO_4 and $\text{Sm}_{1.5}\text{Sr}_{0.5}\text{CuO}_4$, calcined at 1273 K and 1473 K respectively, are shown in Fig. 2. By comparing the patterns with that of other compounds of this series, it can be seen that Sm_2CuO_4 is formed above 1273 K, while there is still a small amount of Sm_2O_3 remained in the $\text{Sm}_{1.5}\text{Sr}_{0.5}\text{CuO}_4$ sample at 1273 K. Thus the formation temperature of the $\text{Sm}_{2-x}\text{Sr}_x\text{CuO}_4$

type compounds is higher than that of the pure Sm₂CuO₄. In order to ensure the formation of all the Sm_{2-x}Sr_xCuO₄ compounds with various x and to get better crystalline, the suitable calcination temperature of 1473 K was suggested.

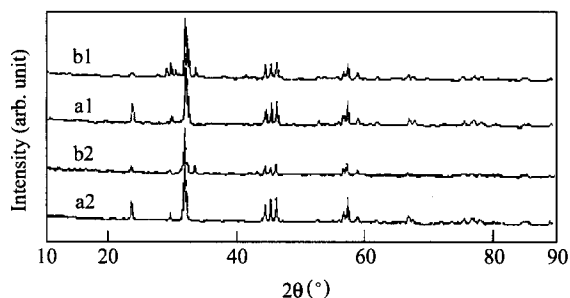


Fig. 2 XRD patterns of Sm₂CuO₄ (a) and Sm_{1.5}Sr_{0.5}CuO₄ (b) at 1372 K (1) and 1472 K (2).

Phase analysis of Sm_{2-x}Sr_xCuO₄ compounds

The XRD patterns of the Sm_{2-x}Sr_xCuO₄ compounds with various x are shown in Fig. 3, and their characteristic peaks are listed in Table 1. From Table 1 it can be seen that these compounds ($0 \leq x \leq 0.6$) are pure single-phase with K₂NiF₄ type structure. When $x = 0.7$ a small amount of Sm₂O₃ phase exists as impurity, when $x \geq 0.8$ the amount of Sm₂O₃ phase increases steadily with the increase of the x value, and when $x = 1.2$ the main phase is no longer attributed by K₂NiF₄ type compound.

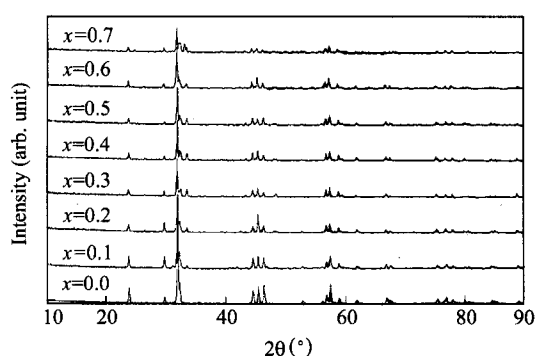


Fig. 3 XRD patterns of the Sm_{2-x}Sr_xCuO₄ compounds with various x .

It is reported that a tolerance factor t ($t = r_{A^+} / \sqrt{2} \cdot r_{B^+}$) is the dominating one to effect the structure type of the K₂NiF₄ compounds.⁶ It is believed that when $0.83 \leq t \leq 0.86$, T' is a unique phase in K₂NiF₄ type compo-

Table 1 Phases and lattice parameters of Sm_{2-x}Sr_xCuO₄ compounds

x	Phase	$a = b$ (nm)	c (nm)
0.0	Sm ₂ CuO ₄	0.39134	1.19681
0.1	Sm _{1.9} Sr _{0.1} CuO ₄	0.39139	1.19718
0.2	Sm _{1.8} Sr _{0.2} CuO ₄	0.39157	1.19795
0.3	Sm _{1.7} Sr _{0.3} CuO ₄	0.39176	1.19851
0.4	Sm _{1.6} Sr _{0.4} CuO ₄	0.39180	1.19872
0.5	Sm _{1.5} Sr _{0.5} CuO ₄	0.39183	1.19892
0.6	Sm _{1.4} Sr _{0.6} CuO ₄	0.39198	1.19931
0.7	Sm _{1.3} Sr _{0.7} CuO ₄ , Sm ₂ O ₃ (slight)	0.39192	1.19942
0.8 ~ 1.2	Sm _{2-x} Sr _x CuO ₄ , Sm ₂ O ₃ , SrO		

unds, while $0.87 \leq t \leq 0.99$, T is a unique phase, and in a narrow range of $0.85 \leq t \leq 0.86$, there exists a T* phase composed of both T and T' phase.

Based on Pauling's ionic radii of the ions in the compound, the tolerance factor of Sm₂CuO₄ is 0.84, and thus the T' type of crystal formed. The ionic radius of Sr²⁺ is larger than that of Sm³⁺, so the substitution of Sm by Sr causes the change of the phase from T' to T. In the compound of T' type, Sm at A position coordinates with 8 oxygen atoms to form octahedral structure, and Cu at B position coordinates with 4 oxygen atoms to form tetragonal structure. The partial substitution of Sr²⁺ for Sm³⁺ results in the defect at the oxygen position as well as in the position A to balance the electric charge. The valence balance can be modified through the defect, which usually results in structural distortion. And the structural distortion hinders further substitution of Sr at position A, so that the excess Sr²⁺ remains as a separate SrO phase.

Table 1 also lists the lattice parameters of Sm_{2-x}Sr_xCuO₄ compounds. It shows that the lattice parameters of these compounds change with the increase of x , because the ionic radius of Sr²⁺ is larger than that of Sm³⁺.

IR spectra of Sm_{2-x}Sr_xCuO₄ compounds is shown in Fig. 4. For comparison, IR spectra of La₂CuO₄ and Pr₂CuO₄ are also given. The former is as a typical T type structure while the latter, a T' type structure.⁶ It is not difficult to distinguish the T type from the T' type according to their IR spectra. For La₂CuO₄, a strong peak at 690 cm⁻¹ is attributed to the stretching vibration of La—O (II) bond at c axis, while the peaks at 520 cm⁻¹ and

375 cm^{-1} , respectively, can be attributed to the stretching vibration and bending vibration of Cu—O(I) bond on a — b plane. For T' type structure such as Pr_2CuO_4 and Sm_2CuO_4 , a peak at 680 cm^{-1} is very weak and becomes strong when x increases, while the peak at 510 cm^{-1} weakened with the increase of x . When $x \geq 0.8$, IR spectra of the $\text{Sm}_{2-x}\text{Sr}_x\text{CuO}_4$ compounds are much more similar to that of La_2CuO_4 other than that of Sm_2CuO_4 . This result is coincident with that of XRD measurement.

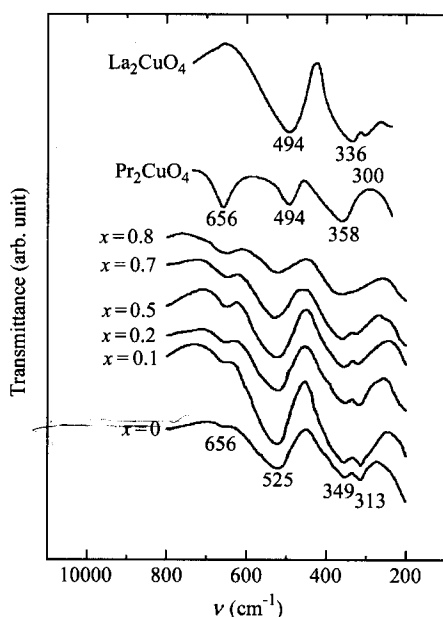


Fig. 4 IR spectra of $\text{Sm}_{2-x}\text{Sr}_x\text{CuO}_4$ compounds.

Structure of $\text{Sm}_{2-x}\text{Sr}_x\text{CuO}_4$ compounds

The powder XRD patterns of the samples can be indexed based on tetragonal symmetry with space group of $I4/mmm$ ($x = 0$ and 0.1). The Rietveld structural refinement of powder diffraction profile of sample at $x = 0$ is shown in Fig. 5, and the corresponding structural parameters are listed in Table 2.

The interatomic distances of the atoms in $\text{Sm}_{2-x}\text{Sr}_x\text{CuO}_4$ compounds ($x = 0.0$ and 0.1) calculated by Rietveld structural refinement are listed in Table 3, and the sum of two relative ionic radii is also listed. Following conclusions can be drawn from Table 3. The distance between Cu and O(II) is shorter than the sum of the ionic radius of Cu^{2+} and O^{2-} , meaning the Cu—O(II) bond in CuO_2 tetragonal plane being contracted. The distance between Sm and O(II) is larger and the distance between

Table 2 Positional and thermal parameters of Sm_2CuO_4 and $\text{Sm}_{1.9}\text{Sr}_{0.1}\text{CuO}_4$

Atom	Site	Parameters	Sm_2CuO_4	$\text{Sm}_{1.9}\text{Sr}_{0.1}\text{CuO}_4$
Sm(Sr)	4e	z	0.3502(1)	0.3508
Sm(Sr)	4e	$B \times 10^2(\text{nm}^2)$	0.39(10)	0.39
Cu	2a	$B \times 10^2(\text{nm}^2)$	0.56(10)	0.56
O(I)	4c	$B \times 10^2(\text{nm}^2)$	1.21(10)	1.21
O(II)	4d	$B \times 10^2(\text{nm}^2)$	0.69(10)	0.69
		R_{wp}	16.01	8.62
Residuals (%)		P_{p}	11.13	6.25
		R_{E}	16.66	5.89
		R_1	13.21	6.14

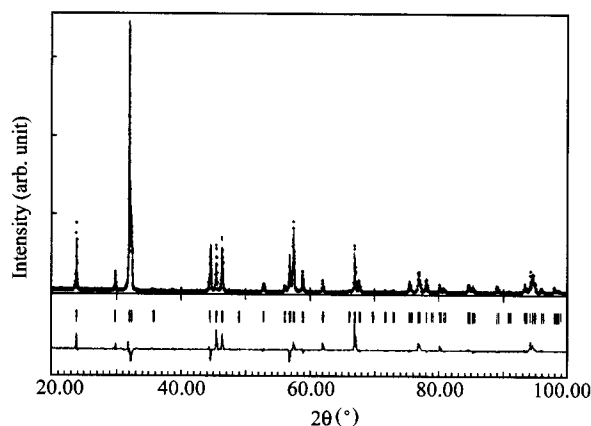


Fig. 5 Rietveld structural refinement of powder diffraction profile of sample $x = 0$. The observed data are indicated by dots and the calculated data by the solid line overlaying them. The short vertical lines mark the positions of possible Bragg reflections and the lower curve shows the difference between the observed and calculated diffraction patterns.

Sm and O(I) is shorter than the sum of the ionic radius of Sm^{3+} and O^{2-} , which means the Sm—O(II) bond stretched and Sm—O(I) bond contracted. When Sr partially substitutes for Sm, the distance between Sm and O(II) becomes shorter, and that between Sm and O(I) becomes longer. It is indicated that the addition of Sr decreases the effective charge at A position. At the same time, the charge at B position does not increase in case of Sr^+ substitution. As a result, a certain amount of defect must be produced at the position of oxygen. According to the characteristics of T' type structure, defect at O(I) position will make the structure more stable than those at O(II) position, and thus the interaction between Sm and O(II) becomes stronger, while the interaction between Sm and O(I) becomes weaker.

The partial substitution of Sr also shortens the Sm—Sm interatomic distance along *c* axis, but slightly lengthens Sm—Sm distance along the *a* axis, meaning that the distance between the two Sm atoms above and beneath the CuO₄ tetragonal plane are contracted. On the other hand, strong electrostatic repellency exists between A-A position, and in order to reduce the repulsion and to stabilize the structure, O(I) moves to A, and A moves to O(II) to decrease the effective charge of A.

Table 3 Interatomic distance (nm) in the compounds Sm₂CuO₄ and Sm_{1.9}Sr_{0.1}CuO₄

Interatomic distance (nm)	<i>x</i> = 0.0	<i>x</i> = 0.1	Sum of ionic radii ^a
Sm—Sm// <i>c</i> axis	0.35856(3)	0.35724(6)	Sr ²⁺ —O ²⁻
Sm—Sm// <i>a</i> axis	0.39134(5)	0.39139(5)	0.256
Sm—O(II)	0.26538(8)	0.26495(2)	Sm ³⁺ —O ²⁻
Sm—O(I)	0.22949(5)	0.22991(1)	0.239
Sm—Cu// <i>c</i> axis	0.27409(1)	0.27397(1)	
Cu—O(II)	0.19567(5)	0.19569(5)	Cu ²⁺ —O ²⁻
Cu—O(I)	0.35750(4)	0.35759(4)	0.208
Bond valence			
Sm	3.15	3.14	
Cu	1.89	1.89	

^aAccording to Pauling's ionic radii. The coordination number for Sm and Sr is 8, for Cu is 4, and for O is 6.

Valence of the metal ions in the Sm_{2-x}Sr_xCuO₄ compounds

The concept of bond-valence has recently found wide application to solid-state chemistry. The main advantage of the approach is that, to an excellent approximation, the bond length may be represented as a unique function of bond valence. The most commonly adopted empirical expression has been proposed for valence calculations as $V_i = \sum_j \nu_{ij} = \sum_j \exp[(R_{ij} - d_{ij})/b]$,¹² in which V_i is the valence of atom *i*, ν_{ij} is the valence of a bond between atom *i* and atom *j*, R_{ij} is the bond-valence parameter, d_{ij} is the bond length of Cu—O(II), Sm—O(I) or Sm—O(II), and *b* is a universal constant (0.037 nm). The R_{ij} parameters for Cu(II)—O and Sm(III)—O are 0.1679 nm and 0.2088 nm, respectively. The calculated V_i values are also listed in Table 3. It can be seen that with the addition of Sr, the bond valence of Cu ions does not increase as expected.

Reducibility of the Sm_{2-x}Sr_xCuO₄ compounds

The TPR results of the Sm_{2-x}Sr_xCuO₄ compounds are shown in Fig. 6. Because the ions of Sm and Sr at A position can not be reduced at the experimental temperature, and hydrogen can only react with the oxygen bonded to Cu²⁺, Cu²⁺ is reduced to lower valences. From Fig. 6, two reduction peaks can be seen. One of them at about 620 °C is attributed to the reaction Cu²⁺ + e → Cu⁺, and the other at higher temperature, to Cu⁺ + e → Cu. The reduction is also dependent on the surroundings of Cu²⁺ ion. When 0.0 ≤ *x* ≤ 0.6, the reduction temperature of Cu²⁺ to Cu⁺ and Cu⁺ to Cu⁰ is almost the same, meaning that the phases of these compounds with *x* ≤ 0.6 are same. However, when *x* ≥ 0.7, some of the Sr which are added stoichiometrically can not enter the lattice of K₂NiF₄ type structure. As a result, a lower TPR peak appears, which may be assigned to the reduction of CuO.

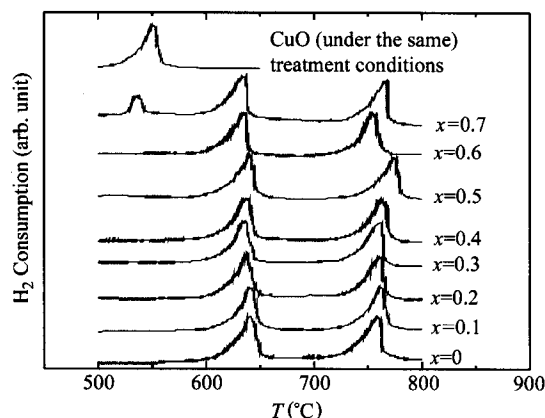


Fig. 6 TPR profiles of Sm_{2-x}Sr_xCuO₄ compounds

Conclusions

Compounds Sm_{2-x}Sr_xCuO₄ (0.0 ≤ *x* ≤ 0.6) with single-phase K₂NiF₄ type structure can be prepared by citric acid complex decomposition method, and the formation temperature is from 1362 K to 1400 K. When *x* ≥ 0.7, free SrO phase and CuO phase appear and gradually become dominant phases. Sm_{2-x}Sr_xCuO₄ are found to belong to tetragonal system of *I4/mmm* space group, and to be of T' type structure, in which Sm or/and Sr coordinates with 6 oxygen ions while Cu at the basal plane coordinates with 4 oxygen ions.

The interatomic distances change with the increasing of Sr substitution, and thus the structure changes accord-

ingly. On the TPR profiles of $\text{Sm}_{2-x}\text{Sr}_x\text{CuO}_4$, there are two reduction peaks which are attributed to the reduction step $\text{Cu}^{2+} + e \rightarrow \text{Cu}^+$ at the lower temperature, and to the reduction step $\text{Cu}^+ + e \rightarrow \text{Cu}$ at the higher temperature.

References

- 1 Ganguly, P.; Rao, C. N. R. *Mater. Res. Bull.* **1973**, *8*, 405.
- 2 Sayer, M.; Odier, P. *J. Solid State Chem.* **1987**, *67*, 26.
- 3 Arbuckle, B. W.; Ramanujachary, K. V.; Zhang, Z.; Greenblatt, M. *J. Solid State Chem.* **1990**, *88*, 278.
- 4 Arbuckle, B. W.; Ramanujachary, K. V.; Buckley, A. M.; Greenblatt, M. *J. Solid State Chem.* **1992**, *97*, 274.
- 5 Lou, H.; Ge, Y.-P.; Chen, P.; Ma, F.-T.; Li, G.-L. *J. Mater. Chem.* **1997**, *7*, 2097.
- 6 Joseph, F. B.; Steven, S. T.; Bruce, A. S. *J. Solid State Chem.* **1990**, *86*, 310.
- 7 Bularzik, J.; Navrotsky, A.; Dicarolo, J. *J. Solid State Chem.* **1991**, *93*, 418.
- 8 Nguyen, N.; Choisnet, J.; Hervieu, M.; Raveau, B. *J. Solid State Chem.* **1981**, *39*, 120.
- 9 He, J.; Sun, Y.-J.; Li, H.; Zang, X.-W.; Zhang, W.-J. *Mol. Catal.* **1994**, *8*, 325 (in Chinese).
- 10 Baythoun, M. S. G.; Sale, F. R. *J. Mater. Sci.* **1982**, *17*, 2757.
- 11 Sakthivel, A.; Young, R. A. *User's Guide to Programs DB-WS-9006*, **1981**.
- 12 Brese, N. E.; O'Keeffe, M. *Acta Crystallogr.* **1991**, *B47*, 192.

(E0106075 LI, L. T.; DONG, H. Z.)